

Reactions of NO with Mn(II) and Mn(III) Centers Coordinated to Carboxamido Nitrogen: Synthesis of a Manganese Nitrosyl with Photolabile NO

Kaushik Ghosh,[†] Aura A. Eroy-Reveles,[†] Belem Avila,[†] Theodore R. Holman,^{*,†} Marilyn M. Olmstead,[‡] and Pradip K. Mascharak^{*,†}

Department of Chemistry and Biochemistry, University of California, Santa Cruz, California 95064, and Department of Chemistry, University of California, Davis, California 95616

Received December 5, 2003

The Mn(II) and Mn(III) complexes of the pentadentate ligand *N,N*-bis(2-pyridylmethyl)amine-*N*-ethyl-2-pyridine-2-carboxamide (PaPy₃H; H is the dissociable carboxamide H), namely, [Mn(PaPy₃)(H₂O)]ClO₄ (**1**) and [Mn(PaPy₃)(Cl)]ClO₄ (**2**), with bound carboxamido nitrogen have been isolated and characterized. The high-spin Mn(II) center in **1** is very sensitive to dioxygen, and this complex is rapidly converted into **2** upon reaction with Cl[−] in air. The bound carboxamido nitrogen in **1** is responsible for this sensitivity toward oxidation since the analogous Schiff base complex [Mn(SBPY₃)Cl]ClO₄ (**4**) is very resistant to oxidation. Reaction of NO with **1** affords the diamagnetic {Mn–NO}⁶ nitrosyl [Mn(PaPy₃)(NO)]ClO₄ (**5**). Complexes with no bound carboxamido nitrogen such as **4** and [Mn(PaPy₃H)(Cl)]₂ (**3**) do not react with NO. No reaction with NO is observed with the Mn(III) complexes **2** and [Mn(PaPy₃)(MeCN)]²⁺ either. Collectively these reactions indicate that NO reacts only with the Mn(II) center ligated to at least one carboxamido nitrogen. Both the carbonyl and N–O stretching frequencies (ν_{CO} and ν_{NO}) of the present and related complexes strongly suggest a {low-spin Mn(II)–NO*} formulation for **5**. The alternative description {low-spin Mn(I)–NO⁺} is not supported by the spectroscopic and redox behavior of **5**. Complex **5** is the first example of a {Mn–NO}⁶ nitrosyl that exhibits photolability of NO upon illumination with low-intensity tungsten lamps in solvents such as MeCN and H₂O. The rapid NO loss from **5** leads to the formation of the corresponding solvato species [Mn(PaPy₃)(MeCN)]²⁺ under aerobic conditions. Oxidation of **5** with (NH₄)₂[Ce(NO₃)₆] in MeCN affords the highly reactive paramagnetic (*S* = 1/2) {MnNO}⁵ nitrosyl [Mn(PaPy₃)(NO)](NO₃)₂ (**6**) in high yield. Spectroscopic and magnetic studies confirm a {low-spin Mn(II)–NO*} formulation for **6**. The N–O stretching frequencies (ν_{NO}) of **5**, **6**, and analogous nitrosyls reported by other groups collectively suggest that ν_{NO} is a better indicator of the oxidation state of NO (NO⁺, NO*, or NO[−]) in non-heme iron and other transition-metal complexes with bound NO.

The reactions of nitric oxide (NO) with transition-metal ions have been studied for quite sometime.¹ In recent years, interactions of NO with iron and copper centers have been explored to model Fe- and Cu-containing metalloenzymes involved in bacterial respiration and denitrification.² Since

manganese is an important metal in biology and is known to participate in redox reactions,³ we were curious about its reactions with NO, a key molecule in biological⁴ and environmental processes.⁵ Although the Mn–NO linkage is well documented in organometallic compounds,^{6–9} and in

* Authors to whom correspondence should be addressed. E-mail: mascharak@chemistry.ucsc.edu (P.K.M.).

[†] University of California, Santa Cruz.

[‡] University of California, Davis.

(1) Richter-Addo, G. B.; Legzdins, P. *Metal Nitrosyls*; Oxford University Press: New York, 1992.

(2) Wasser, I. M.; deVries, S.; Moenne-Loccoz, P.; Schroder, I.; Karlin, K. D. *Chem. Rev.* **2002**, *102*, 1201.

(3) (a) *Manganese and its Role in Biological Processes*; Sigel, A., Sigel, H., Eds. *Met. Ions Biol. Syst.* **2000**, *37*. (b) *Manganese Redox Enzymes*; Pecoraro, V. L., Ed., VCH: New York, 1992.

(4) *Methods in Nitric Oxide Research*; Feilisch, M., Stamler, J. S., Eds.; Wiley: Chichester, U.K., 1996.

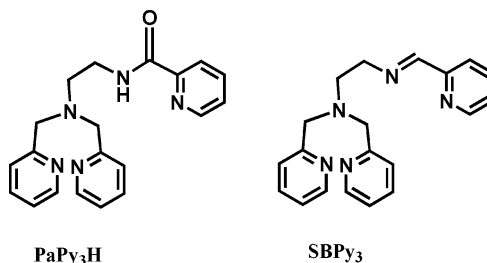
(5) Schwartz, S. E.; White, W. H. J. *Trace Atmospheric Constituents. Properties, Transformation and Fates*; Wiley & Sons: New York, 1983.

porphyrin^{10,11} and phthalocyanine complexes,¹² relatively fewer mononuclear coordination complexes with bound NO are reported so far.^{13–15} Assignment of the formal oxidation states of the manganese center in all these complexes has often been avoided by the use of the {Mn–NO}ⁿ notation of Enemark and Feltham.¹⁶ In selected cases, formal oxidation states have been assigned on the basis of metric, magnetic, and spectroscopic data. For example, Taylor and co-workers have suggested a {low-spin Mn(I)–NO⁺} formulation for the diamagnetic {Mn–NO}⁶ species derived from dianionic pentadentate Schiff base complexes of Mn(II),^{13a} while Lippard and co-workers have assigned a {high-spin Mn(III)–NO⁻} ground state for the {Mn–NO}⁶ tropocoronand complex [Mn(NO)(TC-5,5)] on the basis of FTIR ($\nu_{\text{NO}} = 1662 \text{ cm}^{-1}$) and magnetic ($\sim 4 \mu_{\text{B}}$) parameters.¹⁵ In the case of the diamagnetic {Mn–NO}⁶ tetraphenylporphinato nitrosyl [Mn(TPP)(NO)], a {low-spin Mn(I)–NO⁺} formulation has also been assigned on the basis of the metric parameters (a linear Mn–N–O bond and shorter Mn–N bond distances).^{10b} Interestingly, the Mn–N–O angles in all these species are within the narrow range of 174–180°, and hence, assignment of NO⁺ over NO[•] or NO⁻ on the basis of the Mn–N–O bond angle is not very convincing. On the other hand, the N–O stretching frequency (ν_{NO}) appears to be quite sensitive to the assignment since [Mn(NO)(TC-5,5)] exhibits ν_{NO} at 1662 cm⁻¹ while [Mn(TPP)(NO)] and [Mn-(5-CH₃SALDPT)(NO)] (SALDPT = dianionic pentadentate Schiff base) display ν_{NO} at 1735 and 1715 cm⁻¹, respectively.^{10b,13a,15} The latter ν_{NO} values are close to that of

[Mn(CN)₅(NO)]³⁻ (1725 cm⁻¹), an organometallic species with an effectively Mn(I) center.¹⁷ Although this argument favors the {Mn(I)–NO⁺} formulation for the diamagnetic complexes such as [Mn(TPP)(NO)], controversy still exists in the case of complexes derived from ligands such as the Schiff bases¹³ that are usually not very supportive of metals in low oxidation states. Also, the average Mn–N distance in [Mn(NO)(TC-5,5)], a formally high-spin Mn(III) complex, is 2.00 (3) Å, while that in the Schiff base complex, a formally low-spin Mn(I) species, is 2.06 Å.^{13b} Clearly, the Mn(I)–NO⁺ formulation is not supported by metric data in most cases. Whether the alternative description of {low-spin Mn(I)–NO⁺}, namely, a strongly coupled {low-spin Mn(II)–NO[•]}, is a possibility in such cases remains an open question.

The reactions of the various manganese complexes with NO as well as the reactions of excess NO with the reported manganese nitrosyls are also quite different. For example, Mn(II) complexes of the aforementioned Schiff base ligands (L) react with NO to afford diamagnetic [MnL(NO)] species, while the corresponding Mn(III) complexes of the type [MnLX] (X = I⁻, NCS⁻) react with NO to yield EPR-active high-spin Mn(II) species.¹³ The Mn(II) tropocoronand complex [Mn(THF)(TC-5,5)] reacts with NO to afford [Mn(NO)(TC-5,5)], which reacts further with excess NO to produce N₂O and the nitrito complex [Mn(NO₂)(TC-5,5)].¹⁵ In addition, [Mn(NO)(TC-5,5)] transfers NO to [Fe(TC-5,5)] to produce the {Fe–NO}⁷ nitrosyl [Fe(NO)(TC-5,5)].¹⁸ The Mn(II) porphyrinato complex [Mn(TPP)] reacts readily with NO to afford [Mn(TPP)(NO)],^{10,11} while the corresponding Mn(III) species such as [Mn(TPP)(CN)] reacts with excess NO to yield EPR-active Mn(II) complexes of the type [Mn(TPP)(CN)(NO)].¹¹ This reaction can be reversed by thorough degassing. Reversible coordination of NO to Mn(II) complexes of the type MnX₂(PR₃)₂ (PR₃ = phosphines, X = Cl⁻, Br⁻) in THF solution has also been reported. Collectively, these reactions suggest that NO might have a preference for Mn(II) over Mn(III).

Recently, we have synthesized a designed pentadentate ligand, *N,N*-bis(2-pyridylmethyl)amine-*N*-ethyl-2-pyridine-2-carboxamide (PaPy₃H; H is the dissociable carboxamide



H), in which we have assembled two domains that respectively provide stability to low and high oxidation states of transition-metal ions. For example, the bis(pyridylmethyl)amine portion of PaPy₃H prefers Fe(II),^{19,20} while the

- (6) (a) Enemark, J. H.; Ibers, J. A. *Inorg. Chem.* **1967**, *6*, 1575. (b) Frenz, B. A.; Enemark, J. H.; Ibers, J. A. *Inorg. Chem.* **1969**, *8*, 1288.
- (7) (a) Evrard, G.; Thomas, R.; Davis, B. R.; Bernal, I. *Inorg. Chem.* **1976**, *15*, 52. (b) Messer, D.; Landgraf, G.; Behrens, H. *J. Organomet. Chem.* **1979**, *172*, 349. (c) Potenza, J. A.; Johnson, R.; Rudich, S.; Efraty, A. *Acta Crystallogr., Sect. B* **1980**, *36*, 1933. (d) Sheridan, J. B.; Geoffroy, G. L.; Rheingold, A. L. *J. Am. Chem. Soc.* **1987**, *109*, 1584. (e) Sheridan, J. B.; Johnson, J. R.; Handwerker, B. M.; Geoffroy, G. L.; Rheingold, G. L. *Organometallics* **1988**, *7*, 2404. (f) Nietlispach, D.; Bosch, H. W.; Berke, H. *Chem. Ber.* **1994**, *127*, 2403.
- (8) (a) Laing, M.; Reimann, R. H.; Singleton, E. *Inorg. Chem.* **1979**, *18*, 324. (b) Laing, M.; Reimann, R. H.; Singleton, E. *Inorg. Chem.* **1979**, *18*, 1648. (c) Wilson, R. D.; Bau, R. *J. Organomet. Chem.* **1980**, *191*, 123. (d) Lin, J. T.; Wang, S. Y.; Chou, Y. C.; Gong, M. L.; Shiow, Y.-M.; Gau, H.-M.; Wen, Y. S. *J. Organomet. Chem.* **1996**, *508*, 183.
- (9) (a) Chung, Y. K.; Honig, E. D.; Robinson, W. T.; Sweigart, D. A.; Connelly, N. G.; Ittel, S. D. *Organometallics* **1983**, *2*, 1479. (b) Pike, R. D.; Ryan, W. J.; Carpenter, G. B.; Sweigart, D. A. *J. Am. Chem. Soc.* **1989**, *111*, 8535. (c) Pike, R. D.; Alavosus, T. J.; Hallows, W. H.; Lennhoff, N. S.; Ryan, W. J.; Sweigart, D. A.; Bushweller, C. H.; DiMeglio, C. M.; Brown, J. H. *Organometallics* **1992**, *11*, 2841. (d) Cao, Y.; Woo, K.; Yeung, L. K.; Carpenter, G. B.; Sweigart, D. A. *Organometallics* **1997**, *16*, 178.
- (10) (a) Picuolo, P. L.; Rupprecht, G.; Scheidt, W. R. *J. Am. Chem. Soc.* **1974**, *96*, 5293. (b) Scheidt, W. R.; Hatano, K.; Rupprecht, G. A.; Picuolo, P. L. *Inorg. Chem.* **1979**, *18*, 292.
- (11) (a) Wayland, B. B.; Olson, L. W. *Inorg. Chim. Acta* **1974**, *11*, L23. (b) Wayland, B. B.; Olson, L. W.; Siddiqui, Z. U. *J. Am. Chem. Soc.* **1976**, *98*, 94.
- (12) Goldner, M.; Geniffke, B.; Franken, A.; Murray, K. S.; Homborg, H. *Z. Anorg. Allg. Chem.* **2001**, *627*, 935.
- (13) (a) Coleman, W. M.; Taylor, L. T. *J. Am. Chem. Soc.* **1978**, *100*, 1705. (b) Cooper, D. J.; Ravenscroft, M. D.; Stotter, D. A.; Trotter, J. *J. Chem. Res., Miniprint* **1979**, 3359. (c) Coleman, W. M. *Inorg. Chim. Acta* **1981**, *49*, 205.
- (14) Franceschi, F.; Heschbrouck, J.; Solari, E.; Floriani, C.; Re, N.; Rizzoli, C.; Chiesi-Villa, A. *J. Chem. Soc., Dalton Trans.* **2000**, 593.
- (15) Franz, K. J.; Lippard, S. J. *J. Am. Chem. Soc.* **1998**, *120*, 9034.
- (16) Enemark, J. H.; Feltham, R. D. *Coord. Chem. Rev.* **1974**, *13*, 339.

(17) Cotton, F. A.; Monchamp, R. R.; Henry, R. J. M.; Young, R. C. *J. Inorg. Nucl. Chem.* **1959**, *10*, 28.

(18) Franz, K. J.; Lippard, S. J. *Inorg. Chem.* **2000**, *39*, 3722.

carboxamide portion stabilizes Fe(III) to a significant extent.²¹ As a consequence, this ligand readily affords the low-spin Fe(III) complex [Fe(PaPy₃)(MeCN)](ClO₄)₂ that binds to a variety of ligands (Cl⁻, NO₂⁻, CN⁻) at the sixth site via replacement of the bound solvent molecule.²² This complex also binds NO to afford a diamagnetic {Fe–NO}⁶ nitrosyl [Fe(PaPy₃)(NO)](ClO₄)₂ that rapidly loses NO upon illumination to visible light of low intensity.^{23,24} In addition, one can synthesize [Fe(PaPy₃)(NO)]ClO₄, the corresponding {Fe–NO}⁷ species with an *S* = 1/2 ground state.²⁴ These results have prompted us to study the reactions of NO with manganese complexes of this ligand. In this paper we report a Mn(II) complex, [Mn(PaPy₃)(H₂O)]ClO₄ (**1**), and a Mn(III) complex, [Mn(PaPy₃)(Cl)]ClO₄ (**2**), and their reactions with NO. Two more Mn(II) complexes, namely, [Mn(PaPy₃H)(Cl)₂] (**3**) and [Mn(SBPy₃Cl)]ClO₄ (**4**), that are devoid of coordinated carboxamido nitrogen, and their reactions with NO, are also discussed. The {Mn–NO}⁶ nitrosyl [Mn(PaPy₃)(NO)]ClO₄ (**5**), isolated from the reaction of **1** with NO, and the corresponding {Mn–NO}⁵ species [Mn(PaPy₃)(NO)](NO₃)₂ (**6**) are also described. Synthetic attempts to isolate the diamagnetic {Mn–NO}⁶ nitrosyl **5** have revealed that (a) high-spin Mn(III) shows no affinity for NO and (b) NO binds only to low-spin Mn(II). The Mn(II) nitrosyl **5** also exhibits photolability of the bound NO much like the M(III) nitrosyls [Fe(PaPy₃)(NO)](ClO₄)₂ and [Ru(PaPy₃)(NO)](BF₄)₂.^{23–25} The results described herein demonstrate that unlike the previously reported diamagnetic iron(III) and ruthenium(III) nitrosyls [M(PaPy₃)(NO)]X₂ (M = Fe, Ru; X = ClO₄, BF₄), manganese is in the +2 oxidation state in **5**, and yet all three nitrosyls exhibit photolability of the bound NO ligand.

Experimental Section

2-Aminomethylpyridine, *N*-bromoethylphthalimide, picolinic acid, hydrazine monohydrate, pyridine-2-aldehyde, MnCl₂·4H₂O, and Mn(ClO₄)₂·6H₂O were purchased from Aldrich Chemical Co. and used without further purification. NO gas, procured from Johnson Mathew Chemical Co., was purified by passing it through a KOH column. The starting metal salt [Mn(DMF)₆](ClO₄)₃ was synthesized by following the published procedure.²⁶ All the solvents were purified and/or dried by standard techniques and distilled prior to use. Standard Schlenk techniques were used during all syntheses to avoid exposure to dioxygen. Elemental analyses were performed by Atlantic Microlab Inc.

(19) Patra, A. K.; Olmstead, M. M.; Mascharak, P. K. *Inorg. Chem.* **2002**, *41*, 5403.

(20) (a) Goldsmith, C. R.; Jonas, R. T.; Stack, T. D. P. *J. Am. Chem. Soc.* **2002**, *124*, 83. (b) Roelfes, G.; Lubben, M.; Chen, K.; Ho, R. Y. N.; Meetsma, A.; Genseberger, S.; Hermant, R. M.; Hage, R.; Mondal, S. K.; Young, V. G., Jr.; Zang, Y.; Kooijmann, H.; Spek, A. L.; Que, L., Jr.; Feringa, B. L. *Inorg. Chem.* **1999**, *38*, 1929.

(21) (a) Marlin, D. S.; Olmstead, M. M.; Mascharak, P. K. *Inorg. Chem.* **1999**, *38*, 3258. (b) Marlin, D. S.; Mascharak, P. K. *Chem. Soc. Rev.* **2000**, *29*, 69.

(22) Rowland, J. M.; Olmstead, M. M.; Mascharak, P. K. *Inorg. Chem.* **2001**, *40*, 2810.

(23) Patra, A. K.; Afshar, R.; Olmstead, M. M.; Mascharak, P. K. *Angew. Chem., Int. Ed.* **2002**, *41*, 2512.

(24) Patra, A. K.; Rowland, J. M.; Marlin, D. S.; Bill, E.; Olmstead, M. M.; Mascharak, P. K. *Inorg. Chem.* **2003**, *42*, 6812.

(25) Patra, A. K.; Mascharak, P. K. *Inorg. Chem.* **2003**, *42*, 7363.

(26) Pravakaran, C. P.; Patel, C. C. *J. Inorg. Nucl. Chem.* **1968**, *30*, 867.

CAUTION! Perchlorate salts of metal complexes with organic ligands are potentially explosive. Only small quantities of these compounds should be prepared and handled with proper protection.

Synthesis of the Compounds. The ligands *N,N*-bis(2-pyridylmethyl)amine-*N*-ethyl-2-pyridine-2-carboxamide (PaPy₃H) and *N,N*-bis(2-pyridylmethyl)amine-*N*-ethyl-2-pyridine-2-alimine (SBPy₃) were synthesized according to the literature procedure.^{19,22}

[Mn(PaPy₃)(H₂O)]ClO₄ (1**).** To a solution of 200 mg (0.58 mmol) of PaPy₃H in 15 mL of degassed MeOH was added a batch of 60 mg (0.59 mmol) of Et₃N, and the mixture was stirred for 1 h. A batch of 210 mg (0.58 mmol) of solid Mn(ClO₄)₂·6H₂O was then added, and the mixture was stirred vigorously. A clear pale yellow solution was formed, and within 15 min, a beige precipitate separated out. The precipitate was collected, washed with MeOH, and dried in vacuo (yield 68%). Anal. Calcd for C₂₀H₂₂N₅ClO₆·Mn: C, 46.29; H, 4.24; N, 13.50. Found: C, 46.23; H, 4.22; N, 13.52. Selected IR frequencies (cm⁻¹, KBr disk): 3446 (s, br), 1608 (ν_{CO}), 1591 (vs), 1563 (s), 1372 (s), 1095 (ν_{ClO4}), 755 (s), 622 (s). Value of μ_{eff} (298 K, polycrystal): 5.91 μ_B. X-band EPR spectrum (298 K, polycrystal): strong broad signal with *g* ≈ 2.00.

[Mn(PaPy₃)(Cl)]ClO₄ (2**).** A batch of 15 mg (0.63 mmol) of NaH was added to a solution of 200 mg (0.58 mmol) of PaPy₃H in 15 mL of degassed MeCN, and the reaction mixture was stirred for 1 h. Next, a solution of 459 mg (0.58 mmol) of [Mn(DMF)₆](ClO₄)₃ in 2 mL of MeCN was added to it, and stirring was continued. A green-brown solution was generated within 1 h. At this point, a solution of 97 mg (0.59 mmol) of Et₄NCl in 2 mL of MeCN was added, and the mixture was stirred for another 2 h. The green-brown solution slowly changed to a clear green solution. The solvent was then removed in vacuo, and the green solid was recrystallized from MeCN/Et₂O (yield 62%). Anal. Calcd for [Mn(PaPy₃)(Cl)]ClO₄·2MeCN (2·2MeCN, C₂₄H₂₆N₇Cl₂O₅Mn): C, 46.68; H, 4.21; N, 15.88. Found: C, 46.71; H, 4.17; N, 15.84. Selected IR frequencies (cm⁻¹, KBr disk): 3432 (br), 1638 (vs, ν_{CO}), 1604 (vs), 1447 (s), 1362 (s), 1291 (w), 1083 (vs, ν_{ClO4}), 1020 (s), 764 (s), 623 (s). Electronic absorption spectrum in MeCN, λ_{max} (nm) (ε (M⁻¹ cm⁻¹)): 623 (110), 445 (370), 320 (3400). Value of μ_{eff} (298 K, polycrystal) 5.29 μ_B.

[Mn(PaPy₃H)(Cl)₂] (3**).** A batch of 114 mg (0.58 mmol) of solid MnCl₂·4H₂O was added to a solution of 200 mg (0.58 mmol) of PaPy₃H in 15 mL of degassed MeCN, and the pale yellow solution was stirred for 2 h. Next, the solvent was removed in vacuo, and the pale yellow solid thus obtained was redissolved in 5 mL of MeOH. Slow diffusion of acetone into this solution afforded almost colorless blocks within 72 h (yield 70%). Anal. Calcd for C₂₀H₂₁N₅Cl₂O₂Mn: C, 50.74; H, 4.44; N, 14.80. Found: C, 50.77; H, 4.42; N, 14.78. Selected IR frequencies (cm⁻¹, KBr disk): 3362 (vs, ν_{NH}), 1645 (vs, ν_{CO}), 1605 (s), 1525 (s), 1449 (s), 1425 (s), 1019 (s), 996 (s), 779 (vs), 685 (s). Value of μ_{eff} (298 K, polycrystal) 5.95 μ_B.

[Mn(SBPy₃Cl)]ClO₄ (4**).** A batch of 120 mg (0.61 mmol) of solid MnCl₂·4H₂O was added to a solution of 202 mg (0.61 mmol) of SBPy₃ in 10 mL of degassed MeOH, and the mixture was stirred for 1 h. Next, a batch of 150 mg (1.22 mmol) of solid NaClO₄ was added to the pale yellow solution, and the mixture was stirred for 1 h. The pale yellow solid that separated out was collected by filtration, washed with MeOH, and recrystallized from a CH₂Cl₂/toluene mixture (yield 22%). Anal. Calcd for [Mn(SBPy₃Cl)]ClO₄·0.25MeOH·H₂O (4·0.25MeOH·H₂O, C_{20.25}H₂₄N₅Cl₂O_{5.25}Mn): C, 44.42; H, 4.39; N, 12.80. Found: C, 44.49; H, 4.35; N, 12.77. Selected IR frequencies (cm⁻¹, KBr disk): 3434 (br), 1664 (s), 1606 (vs, ν_{CN}), 1444 (vs), 1306 (s), 1090 (vs, ν_{ClO4}), 759 (s), 623 (s). Value of μ_{eff} (298 K, polycrystal): 5.90 μ_B.

[Mn(PaPy₃)(NO)]ClO₄ (5). A steady stream of purified NO was passed through a suspension of 100 mg of **1** in 10 mL of degassed MeCN in the dark, and the mixture was stirred vigorously. A clear green solution was obtained within 30 min. Next, the passage of NO was stopped, and the solvent was removed in vacuo. The green solid thus obtained was recrystallized from MeCN/Et₂O in the dark (yield 80%). Anal. Calcd for [Mn(PaPy₃)(NO)]ClO₄·2MeCN (**5**·2MeCN C₂₄H₂₆N₈ClO₆Mn): C, 47.02; H, 4.24; N, 18.29. Found: C, 47.09; H, 4.21; N, 18.23. Selected IR frequencies (cm⁻¹, KBr disk): 1745 (vs, ν_{NO}), 1627 (vs, ν_{CO}), 1600 (vs), 1450 (s), 1403 (w), 1090 (vs, ν_{ClO₄}), 766 (s), 623 (s). ¹H NMR (500 MHz, CD₃-CN, δ from TMS): 8.99 (d, 1H), 8.51 (t, 1H), 8.28 (d, 1H), 8.14 (t, 2H), 8.04 (m, 1H), 7.73 (d, 2H), 7.44(t, 2H), 6.72 (d, 2H), 5.02 (dd, 4H), 3.73 (d, 2H), 3.68 (d, 2H). Electronic absorption spectrum in MeCN, λ_{max} (nm) (ε (M⁻¹ cm⁻¹)): 635 (220), 440 (3300), 420 (3320).

[Mn(PaPy₃)(NO)](NO₃)₂ (6). A solution of 145 mg (0.26 mmol) of (NH₄)₂[Ce(NO₃)₆] in 15 mL of MeCN was slowly added to a solution of 132 mg (0.22 mmol) of [Mn(PaPy₃)(NO)]ClO₄ in 10 mL of MeCN, and the mixture was stirred for 30 min. The red-brown solid that precipitated out almost immediately was filtered, washed two times with 5 mL of MeCN, and dried in vacuo (yield 98%). Anal. Calcd for [Mn(PaPy₃)(NO)](NO₃)₂ (**6**, C₂₀H₂₀N₈O₈-Mn): C, 46.80; H, 3.93; N, 13.64. Found: C, 46.72; H, 3.84; N, 13.73. Selected IR frequencies (cm⁻¹, NaCl disk): 3438 (br), 1875 (vs, ν_{NO}), 1622 (vs, ν_{CO}), 1602 (vs), 1471 (s, ν_{NO₃}), 1455 (s, ν_{NO₃}), 1311 (s, br), 1035 (m), 819 (m), 766 (m), 734 (m). Value of μ_{eff} (298 K, polycrystal): 2.22 μ_B.

Conversion of 5 into 2. A batch of 50 mg (0.08 mmol) of [Mn(PaPy₃)(NO)]ClO₄ was dissolved in 15 mL of MeCN in a round-bottom flask, and the green solution was stirred for 1 h in the presence of ordinary light and air. Next, a solution of 15 mg (0.35 mmol) of Et₄NCl in 5 mL of MeCN was added to it, and the mixture was stirred for another 3 h. The volume of the green solution was reduced to 5 mL. Diffusion of Et₂O into this solution afforded crystalline **2** in 60% yield.

Conversion of 1 into 2. A batch of 117 mg (0.21 mmol) of [Mn(PaPy₃)(H₂O)]ClO₄ was suspended in 30 mL of MeCN, and the suspension was stirred in the presence of air. The yellow suspension of the complex first turned brown, and then a clear brown solution was obtained after 6 h. At this point, a solution of 21 μL of 12 N HCl in 5 mL of MeCN was added, and the color sharply changed to deep green. After another hour of stirring, the volume of the solution was reduced to 5 mL. Diffusion of Et₂O into this solution afforded crystalline **2** in 77% yield.

Physical Methods. Electronic absorption spectra of the complexes were recorded on a Cary 50 Varian spectrophotometer. The infrared spectra were obtained with a Perkin-Elmer 1600 FTIR spectrophotometer. ¹H NMR spectra were recorded at 298 K on a Varian 500 MHz spectrometer. A Bruker ELEXSYS E300 spectrometer equipped with a standard cavity and an Oxford Instruments ESR910 flow cryostat was employed to monitor the EPR spectra. Electrochemical measurements were performed with Princeton Applied Research instrumentation. The working electrode was a Beckman Pt-inlay working electrode, and the potentials were measured versus a saturated calomel electrode (SCE).

Photolysis Experiments. The photolysis reactions were studied with the aid of a Cary 50 Varian spectrophotometer. A Varian fiber optics probe was used to monitor the absorbance values at fixed wavelengths for kinetic studies. The tip of the probe was placed inside a 5 dram capped vial containing a ~0.4 × 10⁻³ M solution of **5** (prepared in the dark). Three different solvents (MeCN, DMF, and H₂O) were used. The vial was held at a fixed distance of 5 cm

from tungsten lamps of different powers (25, 60, and 100 W). Periodic scanning of the absorbance values at 440 nm was carried out in the case of MeCN solution, whereas in the cases of DMF and H₂O, the wavelength was held fixed at 450 nm. These wavelengths were chosen to record maximum changes in the absorbance values. Observed rate constant values *K*_{NO} were obtained by fitting the kinetic traces to the equation $A(t) = A_{\infty} + (A_0 - A_{\infty})\{\exp(-K_{NO}t)\}$, where *A*₀ and *A*_∞ are the initial and final absorbance values at fixed wavelength, respectively. The rate constants shown in Table 3 are the mean values of three independent measurements in each case.

X-ray Data Collection and Structure Solution and Refinement. Green blocks of **2**·2MeCN and **5**·2MeCN were obtained by diffusion of Et₂O into solutions of the two complexes in MeCN at 4 °C. Crystals of **3** were obtained by slow diffusion of acetone into a methanolic solution of the complex at room temperature. Orange needles of **4**·0.25MeOH·H₂O were obtained by slow evaporation of a solution of the complex in CH₂Cl₂/toluene. Interestingly, the crystal structure showed the presence of a water molecule in the lattice even after recrystallization from CH₂Cl₂/toluene. Diffraction data were collected at ~90 K (Table 1) on a Bruker SMART 1000 system. Mo Kα (0.71073 Å) radiation was used, and the data were corrected for absorption. The structures were solved by direct methods (standard SHELXS-97 package). The structure of **4**·0.25MeOH·H₂O has two cations in the asymmetric unit, one of which shows disorder. The disorder involves N6, N7, and C21 through C28. These atoms were split into two groups with occupancies of 0.60:0.40 for A:B sets and refined with isotropic thermal parameters. They were also restrained to have the same geometry. One of the two perchlorates was also disordered. It was refined with two sets of oxygen atoms with occupancies 0.53:0.47 for the two sets. Machine parameters, crystal data, and data collection parameters for all the complexes are summarized in Table 1, while selected bond distances and angles are listed in Table 2. Complete crystallographic data for [Mn(PaPy₃)(Cl)](ClO₄)·2MeCN (**2**·2MeCN), [Mn(PaPy₃H)(Cl)₂] (**3**), [Mn(SBPY₃)Cl]ClO₄·0.25MeOH·H₂O (**4**·0.25MeOH·H₂O), and [Mn(PaPy₃)(NO)]ClO₄·2MeCN (**5**·2MeCN) have been submitted as Supporting Information.

Results and Discussion

Reaction of the pentadentate ligand PaPy₃H with Mn-(ClO₄)₂·6H₂O in MeOH (or MeCN) in the presence of 1 equiv of Et₃N affords [Mn(PaPy₃)(H₂O)]ClO₄ (**1**) as a beige precipitate. Elemental analysis, a strong CO stretching frequency (ν_{CO}) at 1608 cm⁻¹, and a strong EPR signal with *g* ≈ 2.00 confirm **1** as a Mn(II) species with bound carboxamido nitrogen.²² Interestingly, in the absence of Et₃N, reaction of MnCl₂·4H₂O with PaPy₃H gives rise to the pentacoordinate Mn(II) complex [Mn(PaPy₃H)(Cl)₂] (**3**) in which PaPy₃H uses only two pyridine nitrogens and the tertiary amine nitrogen to bind the Mn(II) center. The protonated form of the carboxamide group does not participate in coordination. This is readily discernible by the strong and sharp ν_{NH} band at 3362 cm⁻¹ (also in its structure, vide infra). Addition of Et₃N to a solution of **3** in MeCN in air results in a green solution which upon addition of NaClO₄ affords [Mn(PaPy₃)(Cl)](ClO₄) (**2**), a Mn(III) complex with bound carboxamido nitrogen. This hexacoordinated Mn(III) complex is very similar to the Fe(III) complex [Fe(PaPy₃)(Cl)](ClO₄).²² Complex **2** can be conveniently synthesized by starting with the Mn(III) species [Mn(DMF)₆](ClO₄)₃,

Table 1. Summary of Crystal Data and Intensity Collection and Structural Refinement Parameters for **2**·2CH₃CN, **3**, **4**·0.25MeOH·H₂O, and **5**·2CH₃CN

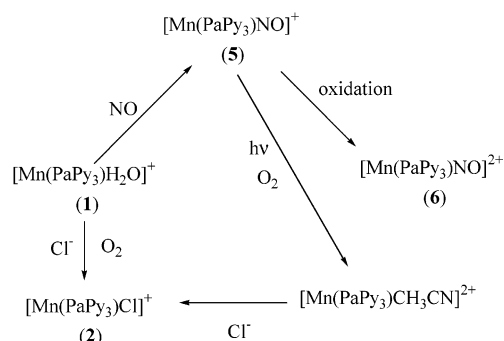
	2	3	4	5
empirical formula	C ₂₄ H ₂₆ N ₇ O ₅ Cl ₂ Mn	C ₂₀ H ₂₁ N ₅ OCl ₂ Mn	C _{20.25} H ₂₄ N ₅ O _{5.25} Cl ₂ Mn	C ₂₄ H ₂₆ N ₈ O ₆ ClMn
fw	618.36	473.26	547.28	612.92
cryst size, mm ³	0.58 × 0.31 × 0.17	0.31 × 0.27 × 0.23	0.71 × 0.22 × 0.66	0.31 × 0.20 × 0.08
cryst color, habit	green, plate	yellow, block	orange, needle	brown, plate
T, K	90(2)	90(2)	93(2)	92(2)
cryst syst	monoclinic	monoclinic	orthorhombic	monoclinic
space group	P2 ₁	P2 ₁ /n	Pna2 ₁	P2 ₁
a, Å	8.5142(19)	13.029(2)	15.161(5)	8.2795(8)
b, Å	14.365(3)	9.2820(17)	11.340(3)	14.0828(14)
c, Å	11.451(3)	18.002(3)	27.053(8)	11.6333(11)
α, deg	90	90	90	90
β, deg	99.483(6)	111.107(3)	90	98.071(2)
γ, deg	90	90	90	90
vol, Å ³	1381.3(5)	2031.0(6)	4651(2)	1343.0(2)
Z	2	4	8	2
density(calcd), g cm ⁻³	1.487	1.548	1.563	1.516
abs coeff, mm ⁻¹	0.719	0.935	0.841	0.647
GOF ^a on F ²	1.033	1.021	1.080	1.030
R1, ^b %	2.04	2.86	6.13	3.00
wR2, ^c %	5.62	6.89	16.60	6.79

^a GOF = $[\sum[w(F_o^2 - F_c^2)^2]/M - N]^{1/2}$ (M = number of reflections, N = number of parameters refined). ^b R1 = $\sum||F_o| - |F_c||/\sum|F_o|$. ^c wR2 = $[\sum[w(F_o^2 - F_c^2)^2]/\sum[w(F_o^2)^2]]^{1/2}$.

Table 2. Selected Bond Lengths (Å) and Angles (deg) for **2**·2CH₃CN, **3**, **4**·0.25MeOH·H₂O, and **5**·2CH₃CN

	2	3	4	5
Mn–N(1)	2.0696(11)	2.3975(13)	2.297(5)	1.9953(15)
Mn–N(2)	1.9133(11)		2.257(5)	1.9551(14)
Mn–N(3)	2.1599(10)		2.409(5)	2.0283(15)
Mn–N(4)	2.2254(11)	2.2244(13)	2.237(5)	2.0336(14)
Mn–N(5)	2.2292(10)	2.2159(13)	2.258(4)	2.0234(14)
Mn–N(6)				1.6601(14)
Mn–Cl(1)	2.2472(4)	2.3459(6)	2.4243(16)	
Mn–Cl(2)		2.4006(6)		
O(1)–C(6)	1.2318(15)			1.244(2)
N(2)–C(6)	1.3445(16)		1.267(7)	1.326(2)
N(3)–C(15)	1.4856(15)		1.498(7)	1.488(2)
N(6)–O(2)				1.1918(18)
N(1)–Mn–N(2)	80.17(4)		70.38(16)	79.45(6)
N(1)–Mn–N(3)	162.59(4)		142.11(16)	162.48(6)
N(1)–Mn–N(4)	100.68(4)	72.72(5)	98.29(17)	96.60(6)
N(1)–Mn–N(5)	105.48(4)	73.23(4)	112.86(17)	98.36(6)
N(1)–Mn–N(6)				95.42(6)
N(1)–Mn–Cl(1)	96.24(3)	94.77(3)	95.26(13)	
N(1)–Mn–Cl(2)		159.75(3)		
N(2)–Mn–N(3)	82.86(4)		74.31(16)	83.19(6)
N(2)–Mn–N(4)	91.39(4)		96.90(16)	89.57(6)
N(2)–Mn–N(5)	86.87(4)		80.99(15)	84.99(6)
N(2)–Mn–N(6)				174.70(7)
N(2)–Mn–Cl(1)	176.24(3)		161.35(13)	
N(3)–Mn–N(4)	75.82(4)		72.55(15)	80.82(6)
N(3)–Mn–N(5)	77.29(4)		73.88(15)	82.40(6)
N(3)–Mn–N(6)				101.88(7)
N(3)–Mn–Cl(1)	100.64(3)		122.00(11)	
N(4)–Mn–N(5)	153.06(4)	116.10(5)	145.60(16)	162.86(5)
N(4)–Mn–N(6)				89.72(6)
N(4)–Mn–Cl(1)	88.14(3)	121.50(4)	96.93(11)	
N(4)–Mn–Cl(2)		97.55(4)		
N(5)–Mn–N(6)				97.13(6)
N(5)–Mn–Cl(1)	95.23(3)	113.73(4)	94.45(12)	
N(5)–Mn–Cl(2)		96.49(3)		
Mn–N(6)–O(2)				171.91(13)
Cl(1)–Mn–Cl(2)		105.394(17)		

PaPy₃H, NaH, and Et₄NCl in MeCN. The affinity of the deprotonated carboxamido group for a M(III) center^{21,22} is clearly evident in the conversion of **3** to **2**. We believe that isolation of **1**, a Mn(II) species with bound carboxamido nitrogen, has only been possible due to its extremely low solubility and lack of other ligands in the reaction mixture.

Scheme 1


Indeed, suspension of **1** in a solvent such as MeCN is very sensitive to air and is readily converted into **2** in the presence of Cl⁻. The extra stability provided by the carboxamido nitrogen to the Mn(III) center in **2** is a major driving force behind this transformation. This is further supported by the fact that the Mn(II) complex of the Schiff base ligand SBPy₃, namely, [Mn(SBPy₃)Cl]ClO₄ (**4**), is very stable and shows no reactivity toward dioxygen.

Passage of NO through a suspension of **1** in degassed MeCN in the dark results in a clear green solution that affords [Mn(PaPy₃)NO]ClO₄ (**5**) in high yield (Scheme 1). This {Mn–NO}⁶ nitrosyl is sensitive to light (vide infra) particularly when in solution. Exposure of a solution of **5** in MeCN ($\lambda_{\text{max}} = 635$ nm) to light under aerobic conditions results in a different green solution ($\lambda_{\text{max}} = 585$ nm) which upon addition of Et₄NCl affords the Mn(III) chloro complex **2** ($\lambda_{\text{max}} = 622$ nm, Scheme 1). It is important to note that NO does not react with manganese in the +3 oxidation state when PaPy₃⁻ is used as the ligand. Thus, direct passage of NO through solutions of [Mn(PaPy₃)(MeCN)]²⁺ (generated either from [Mn(DMF)₆]³⁺ and PaPy₃⁻ or from irradiation of a solution of **5** in MeCN under aerobic conditions) does not afford any nitrosyl species; **5** can only be synthesized from the Mn(II) precursor **1**. The {Mn–NO}⁵ nitrosyl [Mn(PaPy₃)(NO)](NO₃)₂ (**6**) has been isolated as a red-brown solid via oxidation of the {Mn–NO}⁶ nitrosyl **5** with ceric

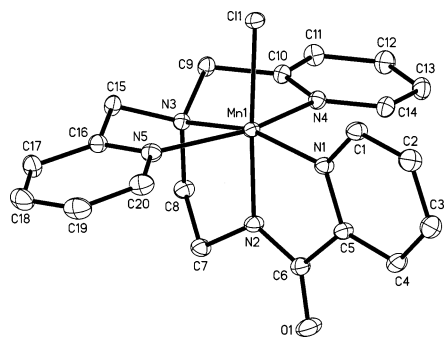


Figure 1. Thermal ellipsoid (probability level 50%) plot of $[\text{Mn}(\text{PaPy}_3)(\text{Cl})]^+$ (cation of **2**) with the atom-labeling scheme. H atoms are omitted for the sake of clarity.

ammonium nitrate in MeCN (Scheme 1). The insolubility of **6** in MeCN allows one to isolate this highly unstable $\{\text{Mn}-\text{NO}\}^5$ nitrosyl in pure form. Complex **6** dissolves in solvents such as DMF and water to afford brown solutions that rapidly turn green, showing reduction to **5**. Although these problems did not allow us to determine the structure of **6** yet, results of physical and analytical measurements have confirmed the structure of this $\{\text{Mn}-\text{NO}\}^5$ nitrosyl.

Structure of the Complexes. $[\text{Mn}(\text{PaPy}_3)(\text{Cl})(\text{ClO}_4) \cdot 2\text{MeCN}]$ (**2**·2MeCN). The structure of $[\text{Mn}(\text{PaPy}_3)(\text{Cl})]^+$ (the cation of **2**) is shown in Figure 1, and the selected bond distances and bond angles are listed in Table 2. The pentadentate monoanionic PaPy_3^- ligand and a Cl^- ion are coordinated to the Mn(III) center in a distorted octahedral geometry. The *tert*-amine and three pyridine nitrogens of the PaPy_3^- ligand comprise the equatorial plane, while the carboxamido nitrogen occupies a position trans to the bound Cl^- ligand. A similar mode of coordination has been observed in the corresponding Fe(III) complex $[\text{Fe}(\text{PaPy}_3)(\text{Cl})]\text{ClO}_4$.²² Comparison of metric parameters of $[\text{Mn}(\text{PaPy}_3)(\text{Cl})]^+$ (Table 2) with those of $[\text{Fe}(\text{PaPy}_3)(\text{Cl})]^+$ however reveals that the metal–ligand bond distances in the Mn(III) complex are significantly longer than those noted for the Fe(III) species. For example, the average Mn(III)– N_{py} (py = pyridine) distance is 2.1747 (11) Å, while the average Fe(III)– N_{py} distance is 1.9862 (16) Å. This arises from the fact that the Mn(III) center in **2** is *high spin* (vide infra) in contrast to the low-spin Fe(III) center in $[\text{Fe}(\text{PaPy}_3)(\text{Cl})]\text{ClO}_4$. Indeed, the Mn(III)– N_{py} , Mn(III)– N_{amine} (2.1599(10) Å), and Mn(III)–Cl (2.2472(4) Å) distances of **2** are comparable to the corresponding distances reported for other high-spin Mn(III) complexes such as $[\text{Mn}(\text{bpia})(\text{Cl})_2]\text{ClO}_4$ (bpia = bis(picolyl)(*N*-methylimidazol-2-yl)amine),²⁸ $[\text{Mn}(\text{bipy})\text{Cl}_3(\text{H}_2\text{O})]$ (bipy = 2,2'-bipyridine),²⁹ and $[\text{Mn}(\text{phen})_2\text{Cl}_2]\text{NO}_3$ (phen = 1,10-phenanthroline).³⁰ Significant deviations from ideal values are observed in the N2–Mn1–Cl1

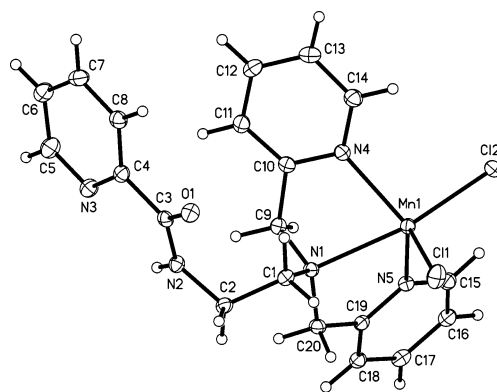


Figure 2. Thermal ellipsoid (probability level 50%) plot of **3** with the atom-labeling scheme.

(176.24(3)°, N1–Mn1–N3 (162.59(4)°), and N4–Mn1–N5 (153.06(4)°) angles of **2** due to ligand constraints.

$[\text{Mn}(\text{PaPy}_3\text{H})(\text{Cl})_2]$ (**3**). As shown in Figure 2, the ligand PaPy_3H in this Mn(II) complex exists in the protonated form, and the carboxamide group and the nitrogen of the pyridine ring attached to it are not coordinated to the metal center. The geometry around the Mn(II) center in this pentacoordinate species is distorted trigonal bipyramidal with two N_{py} atoms and one Cl^- ligand in the basal plane. The free carboxamide–pyridine arm of the ligand stays away from the metal center, and a hydrogen-bonding interaction is noted in the crystal lattice between the hydrogen of the –NHCO– moiety and the carbonyl oxygen of the same moiety from a neighboring molecule (Figure S1, Supporting Information). The two axial donors, namely, N_{amine} and the second Cl^- , are drawn to each other to some extent (N1–Mn1–Cl2 = 159.75(3)°, and both the Mn(II)– N_{py} (2.2244(13) and 2.2159(13) Å) and Mn(II)– N_{amine} (2.3975(13) Å) distances are longer than the corresponding distances noted for the Mn(III) complex **2** (Table 2). Likewise, the Mn(II)–Cl distances (2.3459(6) and 2.4006(6) Å) of this *cis*-dichloro species are also longer than the Mn(III)–Cl (2.2472(4) Å) distance in **2**. The Mn(II)–Cl distances of **3** are however well within the range of Mn(II)–Cl distances reported for similar high-spin Mn(II) complexes.³¹

$[\text{Mn}(\text{SBPy}_3)\text{Cl}]\text{ClO}_4 \cdot 0.25\text{MeOH} \cdot \text{H}_2\text{O}$ (**4**·0.25MeOH·H₂O). The structure of the cation of **4** (Figure 3) resembles that of **2** except for the facts that the pentadentate Schiff base ligand is coordinated to a high-spin Mn(II) center and the Cl^- ligand is trans to an imine nitrogen instead of a carboxamido nitrogen. Consequently, the Mn(II)–Cl (2.4243(16) Å), Mn(II)– N_{amine} (2.409(5) Å), and Mn(II)– N_{py} (2.264(5) Å) distances of **4** are close to the corresponding distances noted for **3** rather than **2**. The Mn(II)– N_{imine} distance (2.257(5) Å) of **4** is close to that noted for other Mn(II) Schiff base complexes.³²

(27) The deep brown solution obtained from oxidation of **1** in MeCN presumably contains a μ -oxodimanganese(III) species. So far, we have not been successful in isolating crystals of this compound. Addition of dilute HCl to this brown solution finally affords **2** in high yield.
 (28) Triller, M. U.; Pursche, D.; Hsieh, W.-Y.; Pecoraro, V. L.; Rompel, A.; Krebs, B. *Inorg. Chem.* **2002**, *41*, 5544.
 (29) Tesouro, A.; Corbella, M.; Stoeckli-Evans, H. *Acta Crystallogr.* **1997**, *C53*, 430.
 (30) Reddy, K. R.; Rajasekharan, M. V. *Polyhedron* **1994**, *13*, 765.

(31) (a) Hubin, T. J.; McCormick, J. M.; Collinson, S. R.; Buchalova, M.; Perkins, C. M.; Alcock, N. W.; Kahol, P. K.; Raghunathan, A.; Busch, D. H. *J. Am. Chem. Soc.* **2000**, *122*, 2512. (b) Oki, A. R.; Bommarreddy, P. R.; Zhang, H.; Hosmane, N. *Inorg. Chim. Acta* **1995**, *231*, 109. (c) Lah, M. S.; Chun, H. *Inorg. Chem.* **1997**, *36*, 1782. (d) Collinson, S.; Alcock, N. W.; Raghunathan, A.; Kahol, P. K.; Busch, D. H. *Inorg. Chem.* **2000**, *39*, 757.

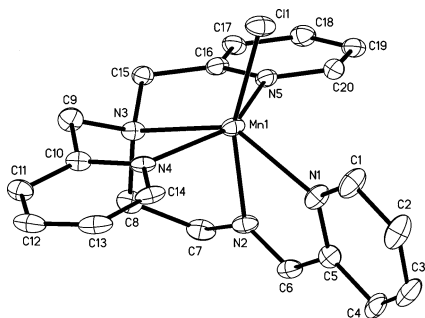


Figure 3. Thermal ellipsoid (probability level 35%) plot of $[\text{Mn}(\text{SBPy}_3)\text{Cl}]^+$ (cation of **4**) with the atom-labeling scheme. H atoms are omitted for the sake of clarity.

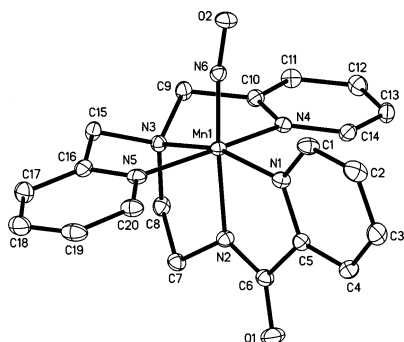


Figure 4. Thermal ellipsoid (probability level 50%) plot of $[\text{Mn}(\text{PaPy}_3)(\text{NO})]^+$ (cation of **5**) with the atom-labeling scheme. H atoms are omitted for the sake of clarity.

$[\text{Mn}(\text{PaPy}_3)(\text{NO})]\text{ClO}_4 \cdot 2\text{MeCN}$ (5**·2MeCN).** The structure of $[\text{Mn}(\text{PaPy}_3)(\text{NO})]^+$ (cation of **5**) is shown in Figure 4, and selected metric parameters are listed in Table 2. In this structure, the metal center is in a distorted octahedral geometry and the *tert*-amine and three pyridine nitrogens of the deprotonated PaPy_3^- ligand comprise the equatorial plane. The carboxamido nitrogen is trans to NO, and the Mn–N–O angle is nearly linear ($171.91(13)^\circ$). Both the Mn–NO ($1.6601(14)$ Å) and N–O ($1.1918(18)$ Å) distances of **5** are comparable to those observed in NO adducts of Mn(II) complexes derived from porphyrins¹⁰ and Schiff bases.^{13b} It is important to note that the Mn–N_{py} and Mn–N_{amine} bond distances of **5** are consistently shorter than the corresponding distances in the Mn(II) complex **4**. For example, in **5**, the Mn–N_{amine} distance is $2.0283(15)$ Å, while the same distance in **4** is $2.273(5)$ Å. This difference clearly indicates the presence of a low-spin Mn(II) center in **5**.

Spectroscopic, Magnetic, and Redox Properties. The presence of a noncoordinated carboxamide group in **3** is readily indicated by the strong ν_{NH} at 3362 cm^{-1} and ν_{CO} at 1645 cm^{-1} . The ν_{CO} value is $\sim 20\text{ cm}^{-1}$ red shifted from the free ν_{CO} value of PaPy_3H (1666 cm^{-1}) due to hydrogen-bonding interactions in the lattice as described above. Complex **1**, on the other hand, exhibits ν_{CO} at 1608 cm^{-1} (and no ν_{NH}), and the red shift of ν_{CO} confirms that the carboxamido nitrogen is bonded to the Mn(II) center.^{21,22} The

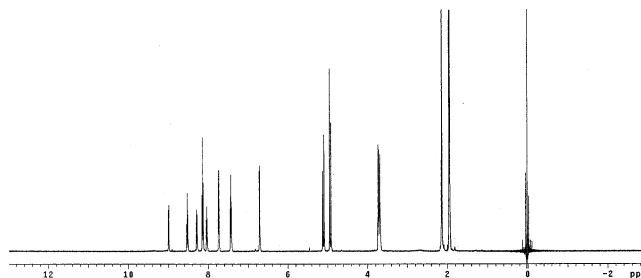


Figure 5. ^1H NMR spectrum (500 MHz) of **5** in CD_3CN (295 K).

Mn(II) centers however exist in the high-spin configuration in both complexes ($\mu_{\text{eff}} = 5.91$ and $5.95\ \mu_{\text{B}}$ for **1** and **3**, respectively). Effects of the bound carboxamido nitrogen are mostly noted in the overall stability of these two species; unlike **3**, complex **1** is more sensitive toward oxygen, is readily oxidized to Mn(III) species such as **2**, and also reacts with NO to afford **5**. In contrast, the high-spin Mn(II) center of the Schiff base complex **4** with no ligated carboxamido nitrogen is very stable in air and does *not* react with NO.³³ Complex **2** also contains a high-spin Mn(III) center ($\mu_{\text{eff}} = 5.29\ \mu_{\text{B}}$). In this regard, the diamagnetism of **5** deserves special attention. The clean NMR spectrum of this nitrosyl (Figure 5) confirms its $S = 0$ ground state, and its IR spectrum exhibits a strong ν_{NO} at 1745 cm^{-1} (KBr disk). This ν_{NO} value is significantly higher than that reported for $[\text{Mn}(\text{TC-5,5})(\text{NO})]$ (1662 cm^{-1}).¹⁵ A Mn(III)–NO[−] formulation has been suggested for the latter complex. Since ν_{NO} values for manganese nitrosyls with formally Mn(II) centers^{10b,13a,17} fall in the range of $1735\text{--}1772\text{ cm}^{-1}$, we have two choices for the electronic description for **5**, namely, {low-spin Mn(I)–NO⁺} and strongly coupled {low-spin Mn(II)–NO[•]}. Since the manganese center of **5** is ligated to a carboxamido nitrogen ($\nu_{\text{CO}} = 1627\text{ cm}^{-1}$), it should be resistant to further reduction.²¹ We therefore prefer the {low-spin Mn(II)–NO[•]} description for the {Mn–NO}⁵ nitrosyl **5**. Indeed, a scrutiny of literature reveals that the {Mn(I)–NO⁺} formulation has often been suggested despite the fact that Mn(II) centers are *not* easily reduced. Electrochemical studies on **5** indicate that this complex is not reduced even at -1.0 V vs SCE. On the other hand, **5** exhibits a quasireversible cyclic voltammogram with $E_{1/2} = 0.9\text{ V}$ vs SCE in MeCN (Figure 6). Chemical oxidation of **5** with ceric ammonium nitrate in MeCN affords the {Mn–NO}⁵ species **6**. Since **6** exhibits ν_{CO} (1622 cm^{-1}) very similar to that of **5** but a very different ν_{NO} (1875 cm^{-1}), it is clear that the oxidant converts the {low-spin Mn(II)–NO[•]} nitrosyl **5** to a {low-spin Mn(II)–NO⁺} nitrosyl **6**. Loss of electron from the antibonding orbital raises ν_{NO} in **5**. More discussion on these assignments is included in a forthcoming section.

The {Mn–NO}⁵ nitrosyl **6** is paramagnetic ($\mu_{\text{eff}} = 2.2\ \mu_{\text{B}}$) and exhibits a low-spin $S = 1/2$ EPR spectrum both in solution and in frozen glass (Figure 7). In DMF solution, **6** exhibits a six-line (^{55}Mn , $I = 5/2$) isotropic EPR spectrum with $g = 1.998$. The observed hyperfine coupling constant (A) value

(32) (a) Ouyang, X.-M.; Fei, B.-L.; Okamura, T.-a.; Sun, W.-Y.; Tang, W.-X.; Ueyama, N. *Chem. Lett.* **2002**, 362. (b) Loulodi, M.; Nastopoulos, V.; Gourbatsis, S.; Perlepes, S. P.; Hadjiliadis, N. *Inorg. Chim. Acta* **1999**, *2*, 479. (c) Nishida, Y.; Tanaka, N.; Yamazaki, A.; Tokii, T.; Hashimoto, N.; Ide, K.; Iwasawa, K. *Inorg. Chem.* **1995**, *34*, 3616.

(33) It is interesting to note here that the Fe(II) complex of SBPy₃, namely, $[\text{Fe}(\text{SBPy}_3)(\text{MeCN})](\text{BF}_4)$, is also very resistant to oxidation although the Fe(II) center exists in a low-spin configuration in this species.¹⁹

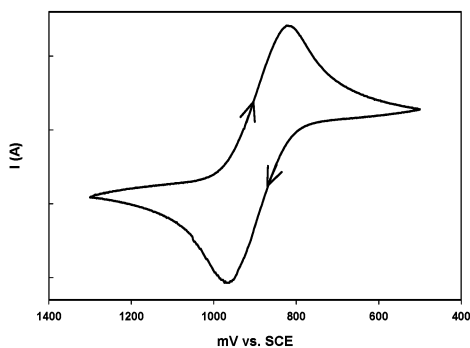


Figure 6. Cyclic voltammogram of **5** in MeCN (Pt electrode, 0.1 M (Et₄N)-(ClO₄), 100 mV/s scan speed). Potentials are indicated vs aqueous SCE.

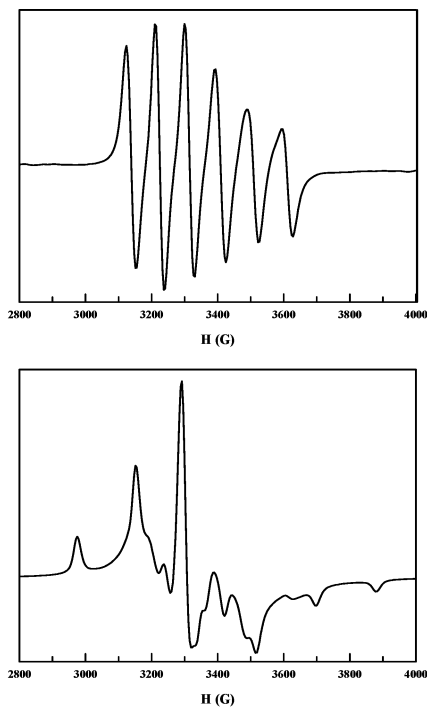


Figure 7. X-band EPR spectrum of **6** in DMF solution (298 K, top panel) and in frozen DMF glass (110 K, bottom panel). Instrument settings: microwave frequency, 9.4187 GHz; power, 31.7 mW; modulation, 100 kHz; modulation amplitude, 2 G.

of 94.6 G lies within the range of 75–100 G reported for other low-spin Mn(II) species.^{34,35} The relatively high *A* value of **6** indicates only a small extent of Mn–ligand back-bonding (PaPy₃[−] is predominantly a σ-donor ligand).³⁴ In frozen glass, **6** displays a well-resolved rhombic spectrum. The three *g* components further split due to hyperfine coupling to give complex spectral features much like the reported low-spin Mn(II) species.^{11,34} At this time, we are trying to determine the values of the various energy parameters from this spectrum. Details will be published elsewhere in conjunction with more structural information on this {Mn–NO}⁵ species.

(34) (a) Saha, A.; Majumdar, P.; Goswami, S. *J. Chem. Soc., Dalton Trans.* **2000**, 1703. (b) Karmakar, S.; Choudhury, S. B.; Chakravorty, A. *Inorg. Chem.* **1994**, *33*, 6148. (c) Basu, P.; Chakravorty, A. *Inorg. Chem.* **1992**, *31*, 4980.

(35) (a) McNeil, D. A. C.; Raynor, J. B.; Symons, M. C. R. *J. Chem. Soc.* **1965**, 410. (b) Manoharan, P. T.; Gray, H. B. *Chem. Commun.* **1965**, 324.

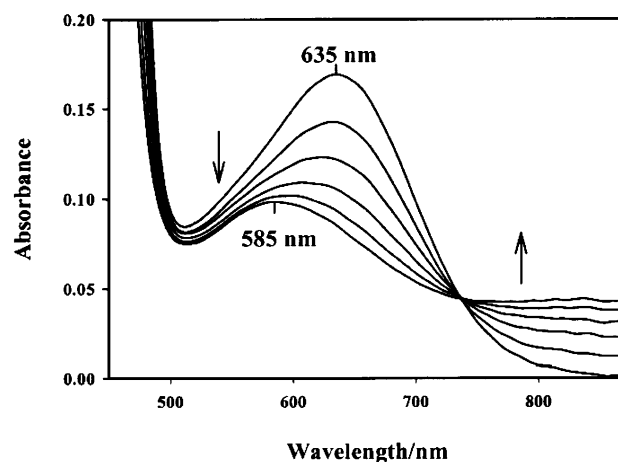
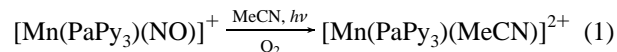


Figure 8. Photodissociation of NO from **5** in MeCN under aerobic conditions (illumination by a 50 W tungsten lamp; concentration of **5**, 0.6 mM; *t*_{1/2} = 52 s).

Light Reactions. Much like the behavior of [Fe(PaPy₃)-(NO)]²⁺ (a {FeNO}⁶ species),²³ exposure of a solution of **5** in MeCN to visible light of low intensity (50 W) results in rapid loss of NO and formation of [Mn(PaPy₃)(MeCN)]²⁺ under aerobic conditions. No loss of NO is noted when the solution is kept in the dark for 48 h. The light-induced NO loss from **5** can be monitored by recording the electronic absorption spectrum of the sample under irradiation. As shown in Figure 8, the conversion of **5** to [Mn(PaPy₃)-(MeCN)]²⁺ in MeCN is evident by the shift of the λ_{max} from 635 nm (value for **5**) to 585 nm. That the final spectrum belongs to [Mn(PaPy₃)(MeCN)]²⁺ has been confirmed by a sample independently synthesized from the reaction of [Mn(DMF)₆](ClO₄)₃ and PaPy₃[−] in MeCN. The clean conversion of **5** into the MeCN-bound (solvated) complex is indicated by the isosbestic points at 735 (Figure 8) and 365 (Figure S2, Supporting Information) nm. No back-reaction (i.e., NO recombination) is observed when the light is turned off since the photoproduct [Mn(PaPy₃)(MeCN)]²⁺, generated under aerobic conditions, is a Mn(III) species with no affinity toward NO. This should be regarded as an advantage with **5** as a photoactive NO donor. As mentioned before, addition of Cl[−] to the photolyzed solution affords complex **2** in good yield.

The light-induced NO loss from **5** (eq 1) follows a pseudo-first-order behavior in solvents such as MeCN, DMF, and H₂O. The value of the NO-off rate constant, *K*_{NO}, increases linearly with the intensity of light (Figure 9). The rate of



NO loss is faster in MeCN compared to that in water (Table 3). Although the *K*_{NO} values of **5** in these solvents are smaller than the *K*_{off} values of the NO adducts of Fe(III) porphyrins,³⁶ one must consider the mild photolysis conditions that have been employed in the case of **5**. The fact that this water-soluble nitrosyl releases NO upon exposure to ordinary light makes it a very good candidate for photodynamic therapy.

(36) Hoshino, M.; Laverman, L.; Ford, P. C. *Coord. Chem. Rev.* **1999**, *187*, 75.

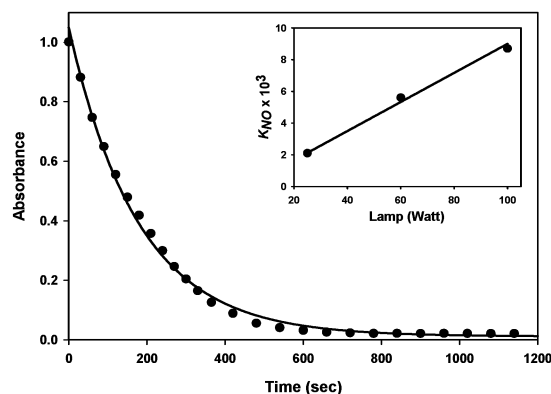


Figure 9. Decrease in absorbance at 450 nm of a solution of **5** in H₂O with time upon illumination (60 W tungsten lamp) and the fit to an exponential function. Inset: K_{NO} values vs the light power (W).

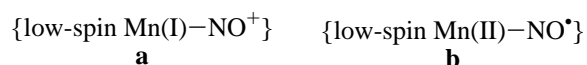
Table 3. Values of K_{NO} of **5** in Different Solvents under Different Light Intensities

solvent	light intensity (W)	$K_{\text{NO}} \times 10^3$ (s ⁻¹)	solvent	light intensity (W)	$K_{\text{NO}} \times 10^3$ (s ⁻¹)
MeCN	25	2.10 ± 0.04	H ₂ O	25	2.10 ± 0.01
	60	7.20 ± 0.01		60	5.60 ± 0.01
	100	15.50 ± 0.01		100	8.70 ± 0.02
DMF	25	1.90 ± 0.01			
	60	6.10 ± 0.03			
	100	13.30 ± 0.02			

We are looking into this possibility in more detail, and the results of such studies will be published in due time.

Electronic Description of the {Mn–NO}⁶ Nitrosyl [Mn(PaPy₃)(NO)](ClO₄) (5**).** In the case of {Mn–NO}⁶ nitrosyls, an almost linear Mn–N–O bond and ν_{NO} in the range 1700–1750 cm⁻¹ are considered as strong evidence for a {low-spin Mn(I)–NO⁺} formulation. This formulation has its origin in the organometallic species [Mn(CN)₅(NO)]³⁻, which exhibits ν_{NO} at 1725 cm⁻¹.¹⁷ What is ignored here is the fact that organometallic species such as [Mn(PR₃)X₂(NO)] (X = Cl⁻, Br⁻) exhibit ν_{NO} in the range 1595–1607 cm⁻¹ and have been assigned a {Mn(III)–NO⁻} formulation.³⁷ Since CN⁻ is a better σ -donor and poorer π -acceptor, the assignment of a {Mn(I)–NO⁺} description for [Mn(CN)₅(NO)]³⁻ seems less probable; the metal center is less likely to accept the single electron on NO in such a species. The same argument holds good for **5**. The PaPy₃⁻ ligand has been repeatedly shown to support high oxidation states of transition metals,^{22–24} and hence, one expects that the manganese center in **5** is more likely to remain in the +2 oxidation state.

Although the two electronic descriptions are just a formalism, we suggest that resonance structure **b** is a better description of the electronic configuration of **5**. The following are the reasons for this choice.



The first evidence in favor of resonance structure **b** is the value of ν_{CO} . Our work has already demonstrated that the

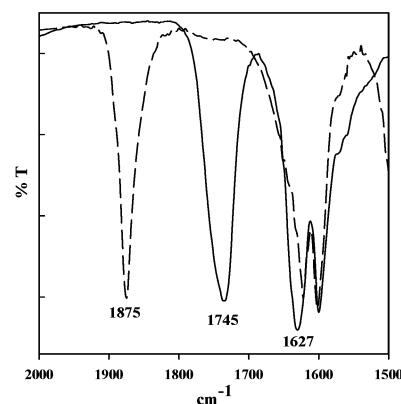


Figure 10. FTIR spectra (2000–1500 cm⁻¹) of **5** (solid line, KBr disk) and **6** (broken line, NaCl disk).

carbonyl stretching frequency is a good indicator of the oxidation states of the metal centers in complexes with a coordinated PaPy₃⁻ ligand. For example, the high-spin Mn(II) complex **1** exhibits its ν_{CO} at 1608 cm⁻¹, while the high-spin Mn(III) complex **2** displays its ν_{CO} at 1638 cm⁻¹. Keeping this in mind, one can easily notice that **5** exhibits its ν_{CO} at 1627 cm⁻¹, a value close to that noted in the case of the {Fe–NO}⁷ species [Fe(PaPy₃)(NO)]ClO₄ (1615 cm⁻¹) for which a {low-spin Fe(II)–NO^{*}} formulation has been confirmed.²⁴ If the resonance structure **a** were the right description of **5**, one would have observed a very different ν_{CO} value for this complex.

The facile NO loss from **5** upon illumination is another piece of evidence in favor of resonance structure **b**. The electronic coupling in the {low-spin Mn(II)–NO^{*}} unit is readily lost upon excitation of an electron from the HOMO; scission of a formally double bond in the case of {Mn(I)–NO⁺} is somewhat unlikely. That the loss of NO from **5** upon illumination leaves a Mn(II) center behind is also confirmed by the following chemical evidence. When a solution of **5** in MeCN is irradiated under strictly anaerobic conditions and then sealed in an EPR tube under vacuum, one monitors a strong EPR signal at $g \approx 2.00$, confirming the presence of Mn(II).³⁸ Addition of Cl⁻ to such a solution does not afford **2**. The trivalent manganese complex **2** is formed only when dioxygen is allowed into the system. Also, since NO does not react with a Mn(III) center, passage of NO through a solution of **5** that has been irradiated in the presence of air does not lead to re-formation of **5**.

Formation of **6** via one-electron oxidation of **5** also supports structure **b** for **5**. Since ν_{CO} does not show any significant change during this oxidation but ν_{NO} does (a change from 1745 to 1875 cm⁻¹, Figure 10), it is apparent that the manganese center does not undergo a change in oxidation state during the **5** → **6** transformation; it is the coordinated NO in **5** that undergoes oxidation to NO⁺ to afford **6**. The alternative scenario in which the oxidant takes away one electron from the Mn(II) center and the {low-spin

(37) Barratt, D. S.; McAuliffe, C. A. *J. Chem. Soc., Chem. Commun.* **1984**, 594.

(38) The NO molecule, following dissociation from **5** upon illumination, can be transferred to reduced myoglobin under this condition (result to be published). This result confirms that the products of the light reaction under anaerobic conditions are [Mn^{II}(PaPy₃)(H₂O)]⁺ (EPR active) and NO.

Mn(III)–NO[•]} intermediate then rearranges into the final {low-spin Mn(II)–NO⁺} product **6** also supports structure **b** for **5**.

Finally, one must note that significant difficulty arises when one tries to assign the oxidation state of manganese in **5** on the basis of the metric parameters. For the complex [Mn(NO)(TC-5,5)] with a {high-spin Mn(III)–NO[−]} formulation, the Mn–N–O angle and the Mn–NO and N–O distances are 174.1(3)°, 1.699(3) Å, and 1.179(3) Å, respectively. In the case of **5**, these values are 171.91(13)°, 1.6601(14) Å, and 1.1918 (18) Å, respectively. Thus, the N–O distance in **5** although close to the N–O distance of free NO (1.15 Å) is longer than that noted for [Mn(NO)(TC-5,5)], a species containing NO[−]! Similar problems arise in the cases of the nitrosylated Mn(II) porphyrinato complexes.¹⁰ These nitrosyls were formally assigned as {low-spin Mn(I)–NO⁺} on the basis of nearly linear Mn–N–O angles and high NO stretching frequencies. However, the Mn–N–O bond angle and Mn–NO and N–O distances of nitrosyl(4-methylpiperidine)(5,10,15,20-tetraphenylporphyrinato)manganese(II) (174.9(6)°, 1.644(5) Å, and 1.176(7) Å, respectively) are practically identical to those of [Mn(NO)(TC-5,5)] with a {high-spin Mn(III)–NO[−]} formulation. Clearly, the metric parameters of these nitrosyls are not good indicators of the oxidation state of the metal centers.

Summary and Conclusions

The following are the principal findings and conclusions of the present study.

(i) One Mn(II) complex and one Mn(III) complex of the pentadentate ligand PaPy₃[−], namely, [Mn(PaPy₃)(H₂O)]ClO₄ (**1**) and [Mn(PaPy₃)(Cl)]ClO₄ (**2**), with bound carboxamido nitrogen have been isolated. The manganese centers in these complexes exist in a high-spin configuration.

(ii) Complex **1** is very sensitive to oxidation and readily converts into **2** in the presence of Cl[−] and dioxygen. The bound carboxamido moiety is responsible for this reactivity since the analogous Schiff base complex [Mn(SBPY₃)Cl]ClO₄ (**4**) is very resistant to oxidation.

(iii) Complex **1** readily reacts with NO to afford the diamagnetic (*S* = 0) {Mn–NO}⁶ nitrosyl [Mn(PaPy₃)(NO)]ClO₄ (**5**). Since both [Mn(PaPy₃)(MeCN)]⁺ and **2** do not show any reactivity toward NO, it is evident that NO reacts only with Mn(II) and not a Mn(III) center. The lack of any reactivity of **4** toward NO also suggests that a bound carboxamido nitrogen is another requirement for the formation of the nitrosyl species.

(iv) **5** is the first example of a {MnNO}⁶ species that exhibits photolability of NO. Spectroscopic and chemical properties support a {low-spin Mn(II)–NO[•]} formulation for **5**.

(v) Oxidation of **5** with (NH₄)₂[Ce(NO₃)₆] in MeCN affords the highly reactive {Mn–NO}⁵ species [Mn(PaPy₃)(NO)](NO₃)₂ (**6**). Spectroscopic and magnetic studies confirm a {low-spin Mn(II)–NO⁺} formulation for this paramagnetic (*S* = 1/2) nitrosyl.

(vi) Assignment of the oxidation states of the metal centers in manganese nitrosyls on the basis of metric parameters leads to ambiguity. In contrast, the NO stretching frequency (ν_{NO}) appears to be a good indicator of the oxidation state of manganese at least in non-porphyrinato complexes. For example, [Mn(NO)(TC-5,5)] with a {high-spin Mn(III)–NO[−]} formulation exhibits ν_{NO} at 1662 cm^{−1}, while **5** with a {low-spin Mn(II)–NO[•]} formulation shows ν_{NO} at 1745 cm^{−1} and **6** with a {low-spin Mn(II)–NO⁺} formulation displays ν_{NO} at 1875 cm^{−1}.

Acknowledgment. Financial support from NIH Grants GM61636 (P.K.M.) and GM56062 (T.R.H.) is gratefully acknowledged.

Supporting Information Available: Hydrogen-bonding interactions in solid **3** (Figure S1), electronic absorption spectra (800–300 nm) showing photodissociation of NO from **5** under aerobic conditions (Figure S2), and X-ray crystallographic data (in CIF format) and tables for the structure determination of complexes **2**·2MeCN, **3**, **4**·0.25MeOH·H₂O, and **5**·2MeCN. This material is available free of charge via the Internet at <http://pubs.acs.org>.

IC030331N